

# The rapid secondary electron imaging system of the proton beam writer at CIBA

C.N.B. Udalagama \*, A.A. Bettiol, J.A. van Kan, E.J. Teo, F. Watt

*Centre for Ion Beam Applications, Department of Physics, National University of Singapore, 2 Science Drive 3, Singapore 117542, Singapore*

Available online 18 April 2007

## Abstract

The recent years have witnessed a proliferation of research involving proton beam (p-beam) writing. This has prompted investigations into means of optimizing the process of p-beam writing so as to make it less time consuming and more efficient. One such avenue is the improvement of the pre-writing preparatory procedures that involves beam focusing and sample alignment which is centred on acquiring images of a resolution standard or sample. The conventional mode of imaging used up to now has utilized conventional nuclear microprobe signals that are of a pulsed nature and are inherently slow. In this work, we report the new imaging system that has been introduced, which uses proton induced secondary electrons. This in conjunction with software developed in-house that uses a National Instruments DAQ card with hardware triggering, facilitates large data transfer rates enabling rapid imaging. Frame rates as much as 10 frames/s have been achieved at an imaging resolution of  $512 \times 512$  pixels.

© 2007 Elsevier B.V. All rights reserved.

PACS: 07.05.Hd; 79.20.Hx; 42.30.Va; 41.85.Lc; 85.40.Hp

Keywords: Data acquisition; Secondary electrons; Rapid imaging; p-Beam writing

## 1. Introduction

Proton beam (p-beam) writing is a novel adaptation of conventional nuclear microprobe technology to create a lithography technique able to produce smooth, 3D structures with high verticality [1]. The last decade has witnessed a proliferation of research involving p-beam writing. These range from projects in metallic stamps/molds [2], photonics [3], micro/nano-fluidics [4], bioapplication [5], resolution standards [2] to the use of p-beam writing of silicon to produce micromachined surfaces [6], patterned porous silicon [7] and patterned Bragg reflectors [8]. This has led to an increase in the demand of the p-beam writer at the Centre for Ion Beam Applications (CIBA), National University of Singapore. It has thus become necessary to optimize typical

procedures for efficiency so as to maximize throughput. One such identified avenue for improvement is the incorporation of a real-time imaging system to expedite the pre-writing preparatory procedures that involve beam focusing and sample alignment. This article presents details of such a rapid imaging system based on proton induced secondary electrons. This system is the same as that mentioned previously in connection with automatic beam focusing [9], introduced at CIBA.

The conventional mode of imaging adopted with the p-beam writer involves the use of the data acquisition (DAQ) system, OMDAQ [10] along with RBS, STIM or proton induced secondary electron (PISE) signals. OMDAQ operates with pulsed signals as inputs and is meant for low countrate (<5 kHz) experiments due to issues of deadtime. This is incompatible with a rapid imaging system [11] owing to: (1) delays inherent in counting pulses and (2) the large data flowrates encountered. For instance, a typical imaging system operating at 10 frames/s at a  $512 \times 512$  pixel resolution requires data from

\* Corresponding author.

E-mail address: [phycnbu@nus.edu.sg](mailto:phycnbu@nus.edu.sg) (C.N.B. Udalagama).

URL: [www.ciba.nus.edu.sg](http://www.ciba.nus.edu.sg) (C.N.B. Udalagama).

a pixel to be analyzed within an interval of the order of 350 ns. This requires a pulsed signal to have its pulse width smaller than this value which translates to a count rate of at least 2.6 MHz. In view of this, we have developed an independent rapid imaging system based on voltage-modulated dc signals. The use voltage-modulated dc signals for imaging has not been preferred [11] with nuclear microprobes due to the significant fluctuations in beam intensity encountered. It has been shown by Takai et al. [12] that fluctuations as small as 0.4–1.7% can be detrimental to the quality of the image. However, the HVEE Singletron ion accelerator at CIBA exhibits a higher degree of beam stability [13] that makes imaging using voltage-modulated dc signals feasible. The present paper, which is a continuation of the previous work by Teo et al. [14], reports the new imaging system which will henceforth be referred to as DAQImaging. It has been implemented using the PCI-6111, PC DAQ card from National Instruments [15]. This card's ADCs perform analogue-to-digital (ADC) conversions within an interval of 200 ns. Another parameter that is as significant as the ADC rate is the digital-to-analogue (DAC) conversion rate. The PCI-6111 has a maximum DAC rate of 2.5 MegaSample/s for two output channels. This allows the generation of the  $(x,y)$  scanning signal for beam movement, at a rate sufficient for image acquisition

at the said 10 frames/s. The detector system is described next.

## 2. DAQ setup

### 2.1. Detector setup

Fig. 1 is a schematic representation of the imaging setup and is similar to that found in [11]. It is based on attracting the PISE from the target. The system includes a cage and biasing ring, that are at positive potentials, attached to a glass tube which in our chamber is made of quartz but can also be of plastic glass. The cage first attracts the secondary electrons from the target which are then accelerated by the ring to impinge on a P-47 powder scintillator. The generated luminescence is then coupled via the quartz tube to a photomultiplier tube (Hamamatsu H3165-10) whose output current is amplified and converted into a voltage by the 'photomultiplier electronics' which is a Hamamatsu C2791 current-to-voltage amplifier. This voltage is fed into the ADC on the NI PCI-6111 PC DAQ card. The DAC (digital-to-analogue converter)s from the card are routed to the scan amplifier which drives the scan coils that enable beam scanning. This imaging system is housed in the p-beam writer which is described in [16].

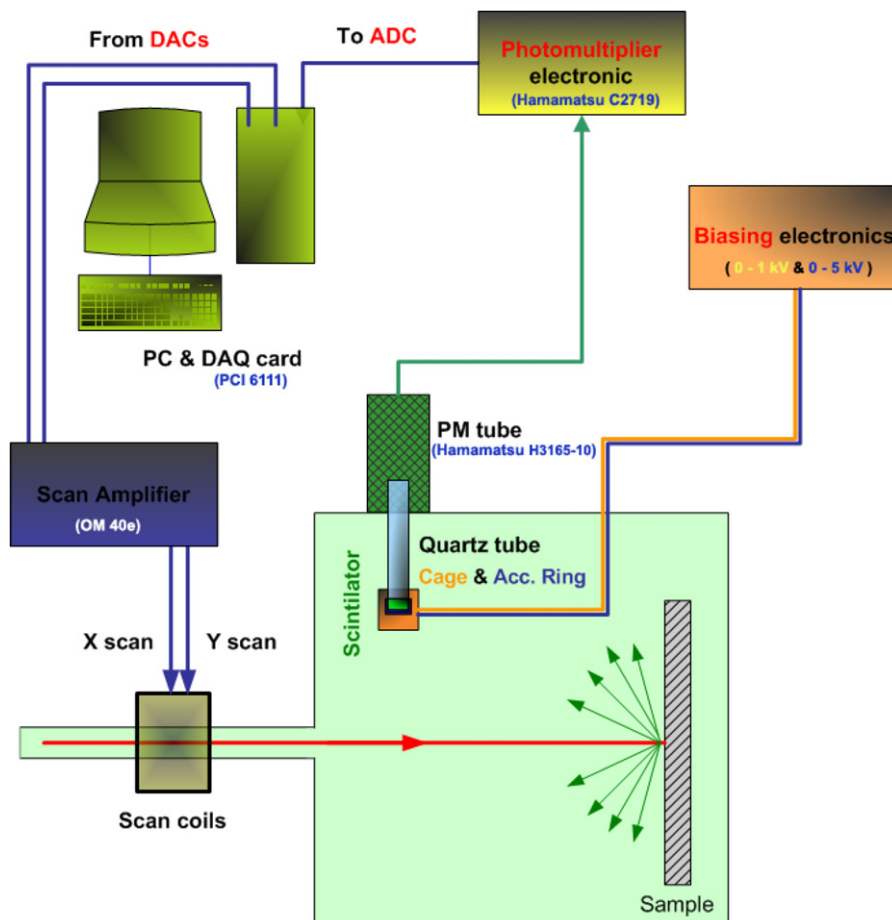


Fig. 1. The experimental setup for the rapid imaging system using PISE.

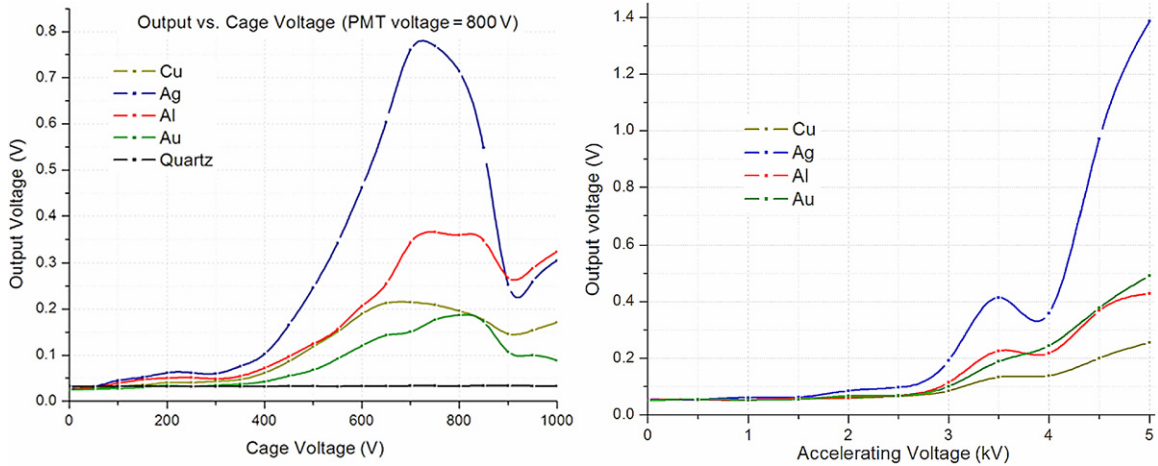


Fig. 2. Dependence of the output signal strength on the acceleration and cage, bias voltages measured with different targets. Note the sparseness of secondary electrons from quartz, due to it being an insulator. Left: varying the cage voltage (beam current  $\approx 1$  pA, accelerating voltage = 5 kV). Right: varying the accelerating voltage. Notice the hump at 3.5 kV (beam current  $\approx 1$  pA, cage voltage = 700 V).

2.2. Detector characteristics

The dependence of the detector output voltage on the cage and accelerating voltages are shown in Fig. 2. We are as yet unable to explain the existence of the observed peaks. However, the observed peaks in connection with the cage voltage have been identified as been related to an increase in the spatial collection of secondary electrons [17]. In accordance with these observations a cage voltage of 700 V and the maximum available accelerating voltage of 5 kV was used in all imaging experiments.

3. Results/features

DAQImaging was developed at CIBA using the C++ programming language in the 2003.Net [18] environment utilizing the National Instruments NIDAQ and IMAQ libraries for data acquisition, beam control and data presentation. Some libraries from numerical recipes in C++ [19] were also used for some of the mathematical routines.

DAQImaging offers many improvements over the pulsed imaging system. Namely: (1) greater imaging resolution ( $>512 \times 512$  pixels), (2) imaging rates up to 10 frames/s at a  $512 \times 512$  pixel resolution, (3) automatic FWHM deconvolution by fitting, (4) image averaging (pixel, line and frame), (5) defining unrestricted linescans, (6) bipolar and unipolar scanning and (7) magnifications of  $\times 2$ ,  $\times 4$  and  $\times 8$ , while still maintaining the original pixel resolution. The details of the implementation of some of these features are provided below. Details of the other features can be found in [17].

3.1. Fast data acquisition through triggering

An imaging system follows the algorithm of repeatedly: (1) moving the beam to a  $(x,y)$  pixel coordinate on the target, (2) dwelling for a fixed time and (3) collecting the sig-

nal strength relevant to this point. As discussed in [17], a purely software implementation of these steps are inadequate in rapid imaging systems as the PC OS latencies upset the microsecond synchrony necessary between the

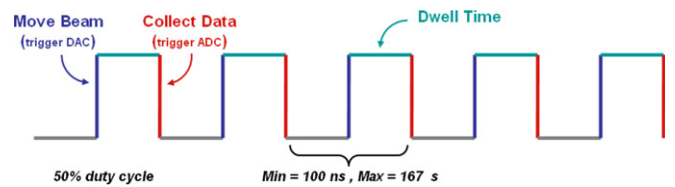


Fig. 3. The timing sequence used in the hardware triggering of DAQImaging. DAC conversion that realizes beam motion is activated on the rising edge of the pulse. The beam is then held stationary until the falling edge of the pulse upon which the ADC conversion is initiated which registers the intensity of the signal. We generate this triggering signal using one of the counters on the PCI-6111 PC DAQ card.

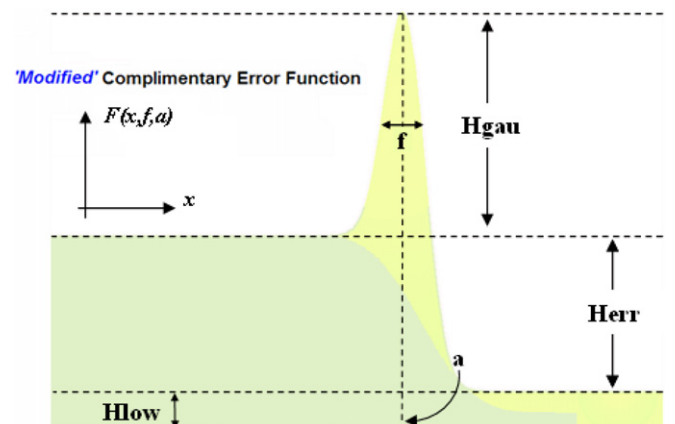


Fig. 4. The fitted parameters in the non-linear fit for the deconvolution of the FWHM of the beam. The light shade corresponds to the contribution from the enhanced edge emission from secondary electrons, while the darker shade is the usual complimentary error function resulting from scanning the beam over a sharp edge.

DAC (for beam movement) and the ADC (for data collection). DAQImaging circumvents this problem by using a square waveform to trigger the DAC and ADC operations. The timing relation is shown in Fig. 3, where the beam is moved (DAC operation) on the rising edge of the pulse and the signal is sampled (ADC operation), from the corresponding  $(x,y)$  position, on the falling edge. The refilling/emptying of the scan/data buffers from PC RAM is accomplished utilizing the NIDAQ DAQ EVENT MES-

SAGING feature that National Instruments DAQ cards and drivers (NIDAQ) offer. This allows the DAQ card to initiate the filling/emptying operations of the buffers.

### 3.2. Averaged image acquisition

DAQImaging is able to incorporate an averaging feature, while collecting the data for imaging. The possible averaging options are *Pixel*, *Line* or *Frame*. This averaging

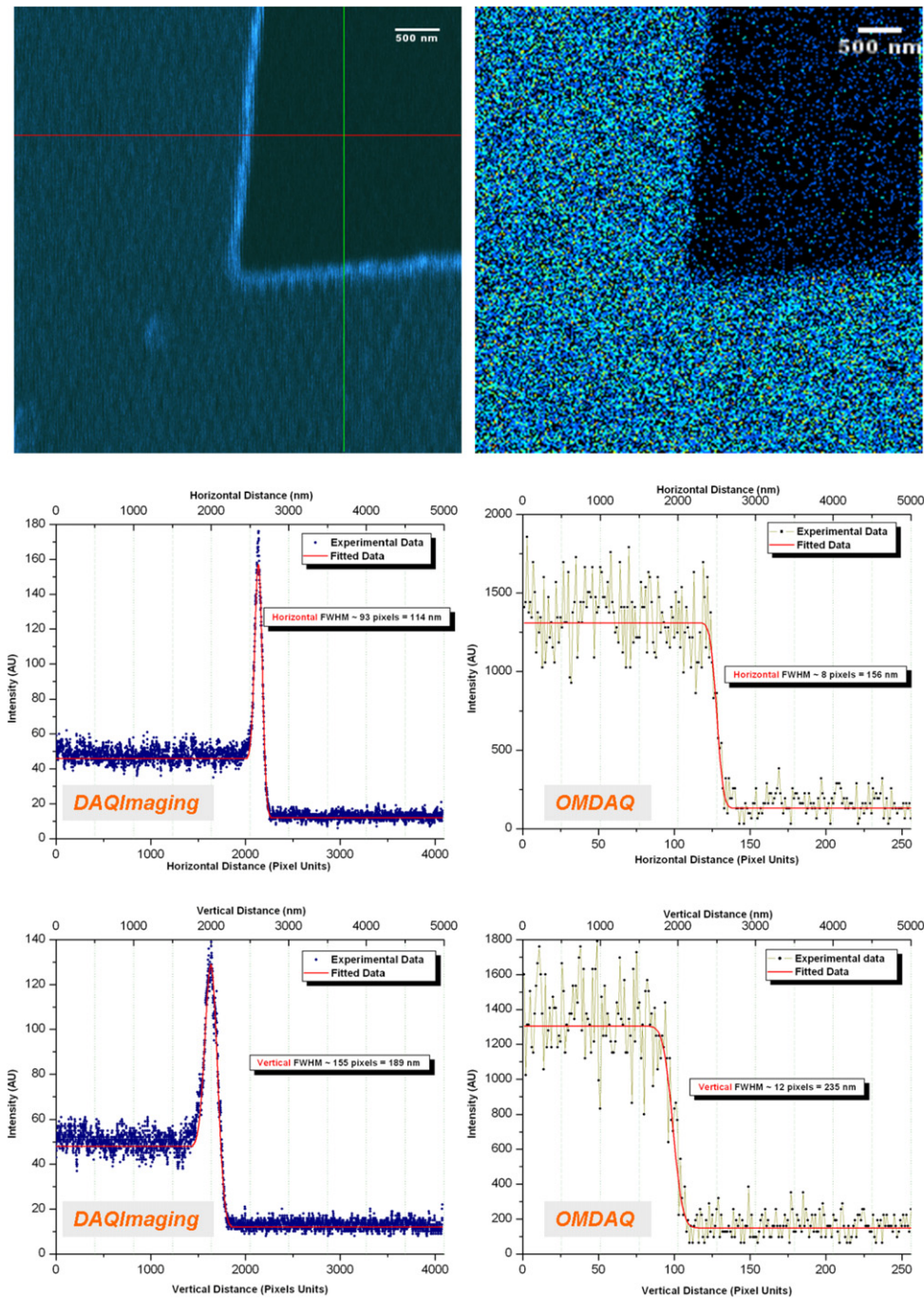


Fig. 5. Comparing DAQImaging with OMDAQ. Beam deconvolution using the same region of nickel grid using the two systems. Left: results for DAQImaging that has greater pixel resolution and an automatic, real-time non-linear fitting routine. Values extracted from the fits: horizontal FWHM  $\approx 93$  pixels = 114 nm, vertical FWHM  $\approx 155$  pixels = 189 nm; Right: results for OMDAQ that has only  $256 \times 256$  pixels and the fitting need to be performed off line. Values extracted from the fits: horizontal FWHM  $\approx 8$  pixels = 156 nm, vertical FWHM  $\approx 12$  pixels = 235 nm.

refers to how the system collects data so as to assign an intensity to the pixels in the image. If one opted for  $n$  averages then the system will, in all averaging modes, use  $n$  values to obtain an average for each pixel. However, the averaging modes differ in how these  $n$  values are collected. For *Pixel* averaging the beam is held stationary at each pixel until the required  $n$  samples are acquired. In *Line* averaging each line of the image is scanned  $n$  times until the  $n$  samples for each of the pixels of that line are collected. In *Frame* averaging the complete frame is scanned  $n$  times. The possible values for  $n$  must be powers of 2, i.e.  $2, 2^2, 2^3, 2^4, \dots$  up to a maximum of 512.

These averaging features are useful if one deals with beam intensity or energy fluctuations [12]. This is particularly relevant to imaging using electrons due to their high sensitivity. Such beam related anomalies have significant effect on the quality of the produced images.

### 3.3. Magnified image acquisition

This feature allows user defined sub-square region-of-interests to be imaged at the original pixel resolution thereby affecting a magnification. The possible sizes of the allowed square regions of interest are  $\frac{1}{2}, \frac{1}{4}$  or  $\frac{1}{8}$  of the scan area, corresponding to the allowed magnification settings  $\times 2, \times 4$  and  $\times 8$ . This feature has been achieved by increasing the imaging pixel resolution beyond  $512 \times 512$  (if necessary, DAQImaging is able to image at a pixel resolution as high as  $4096 \times 4096$ ). By so increasing the resolution it is possible to image smaller regions, while retaining the original pixel resolution. For instance, a choice of  $\times 4$  will mean that the system will scan the image at a pixel resolution of  $2048 \times 2048$ , thereby collecting the required  $512 \times 512$  necessary for magnification.

### 3.4. Beam FWHM deconvolution

Upon specifying two appropriate linescans the imaging software is able to implement a non-linear fit, using the Levenberg–Marquardt method [19], to affect the deconvolution of the beam's FWHM. The actual function used for fitting is given below and takes account of the enhanced edge emission that is a feature of the secondary electron signal [9,17]. The five fitted parameters are **a**, **Herr**, **Hgau**, **Hlow** and **f** which are described in Fig. 4

$$F(x, f, a) = \mathbf{Herr} \left[ 1 + \operatorname{Erf} \left( \frac{2\sqrt{\ln 2}}{\mathbf{f}} (\mathbf{a} - x) \right) \right] + \mathbf{Hgau} \exp \left[ -\frac{\ln 16}{\mathbf{f}^2} (\mathbf{a} - x)^2 \right] + \mathbf{Hlow}.$$

#### 3.4.1. Comparing FWHM deconvolution from RBS and secondary electrons signals

Fig. 5 shows two maps of the same region of a high resolution nickel standard [20]. One has been imaged through

OMDAQ using RBS as the signal, while the other with DAQImaging. Also shown are linescans used for evaluating the beam size. DAQImaging fits and deconvolutes the beam size in real time by using a much greater number of points than OMDAQ. Beam deconvolution for the data from OMDAQ needs to be performed separately.

## 4. Discussion, summary and future work

As a step towards expediting the typical preparatory steps in p-beam writing experiments, a new rapid imaging DAQ system, DAQImaging, has been introduced. DAQImaging is based on utilizing voltage-modulated dc signal from PISE and is able to achieve imaging rates as much as 10 frames/s at a pixel resolution of  $512 \times 512$ . The system achieves these rates by circumventing PC OS latencies, that may affect timing synchrony between DAC and ADC operations, by utilizing a square waveform to affect hardware triggering. In addition the DAQImaging offers improved software features such as unrestricted linescans, magnification, beam deconvolution by non-linear fitting and averaged image acquisition.

At present the use of DAQImaging conveniently and at its full potential is deterred by: (1) the small solid angle of the present detector setup, (2) the low bandwidth imposed by the present current-to-voltage converter and (3) the difficulties encountered in having a highly light sensitive photomultiplier element in the system. This, in addition to requiring the operator to exercise great caution, forces DAQImaging to be used with relatively large ( $\approx 10$  pA) currents and slow frame rates. Avenues of future work being considered currently aim at improving these aspects.

## Acknowledgement

The authors wish to acknowledge the financial support of the United States Air Force (Project A-06046163).

## References

- [1] J.A. van Kan, A.A. Bettiol, F. Watt, Appl. Phys. Lett. 83 (2003) 1629.
- [2] J.A. van Kan, P.G. Shao, P. Molter, M. Saumer, A.A. Bettiol, T. Osipowicz, F. Watt, Nucl. Instr. and Meth. B 231 (2005) 170175.
- [3] A.A. Bettiol, T.C. Sum, F.C. Cheong, C.H. Sow, S.V. Rao, J.A. van Kan, E.J. Teo, K. Ansari, F. Watt, Nucl. Instr. and Meth. B 231 (2005) 364.
- [4] K.A. Mahabadi, I. Rodriguez, S.C. Haur, J.A. van Kan, A.A. Bettiol, F. Watt, J. Micromech. Microeng. 16 (2006) 1070.
- [5] F. Zhang, F. Sun, J.A. van Kan, P.G. Shao, Z. Zheng, R.W. Ge, F. Watt, Nucl. Instr. and Meth. B 231 (2005) 413.
- [6] E.J. Teo, M.B.H. Breese, E.P. Tavernier, A.A. Bettiol, F. Watt, M.H. Liu, D. Blackwood, Appl. Phys. Lett. 84 (2004) 3202.
- [7] E.J. Teo, M.B.H. Breese, A.A. Bettiol, D. Mangaiyarkarasi, F. Champeaux, F. Watt, D. Blackwood, Adv. Mater. 18 (2006) 51.
- [8] D. Mangaiyarkarasi, M.B.H. Breese, Y.S. Ow, C. Vijila, Appl. Phys. Lett. 89 (2006) 021910.
- [9] C.N.B. Udalagama, A.A. Bettiol, J.A. van Kan, E.J. Teo, M.B.H. Breese, T. Osipowicz, F. Watt, Nucl. Instr. and Meth. B 231 (2005) 389.
- [10] G.W. Grime, M. Dawson, Nucl. Instr. and Meth. B 89 (1994) 223.

- [11] L.C. Alves, M.B.H. Breese, M.F. da Silva, J.C. Soares, Nucl. Instr. and Meth. B 188 (2002) 146.
- [12] M. Takai, Y. Agawa, K. Ishibashi, K. Hirai, S. Namba, K. Inoue, Y. Kawata, Nucl. Instr. and Meth. 54 (1991) 279.
- [13] D.J.W. Mous, R.G. Haitzma, T. Butz, R.-H. Flaggmeyer, D. Lehmann, J. Vogt, Nucl. Instr. and Meth. B 130 (1997) 31.
- [14] E.J. Teo, M.B.H. Breese, A.A. Bettiol, F. Watt, J. Vac. Sci. Technol. B 22 (2004) 560.
- [15] National Instruments. <<http://www.ni.com>>.
- [16] J.A. van Kan, A.A. Bettiol, F. Watt, Mat. Res. Soc. Symp. Proc. 777 (2003) T2.1.1.
- [17] C.N.B. Udalagama, Optimization and computer control of the sub-100 nm, proton beam writing facility at CIBA, Ph.D. Thesis, National University of Singapore, 2005.
- [18] Microsoft.net. <<http://www.microsoft.com/net/default.aspx>>.
- [19] W.H. Press, S.A. Teukolsky, W.T. Vetterling, B.P. Flannery, Numerical Recipes in C++, second ed., Cambridge University Press, The Edinburgh Building, Cambridge CB2 2RU, UK, 2002, ISBN 0 521 75033 4.
- [20] F. Zhang, J.A. van Kan, S.Y. Chiam, F. Watt, Nucl. Instr. and Meth. B, these Proceedings, doi:10.1016/j.nimb.2007.02.065.